Journal of Materials Chemistry C

Accepted Manuscript

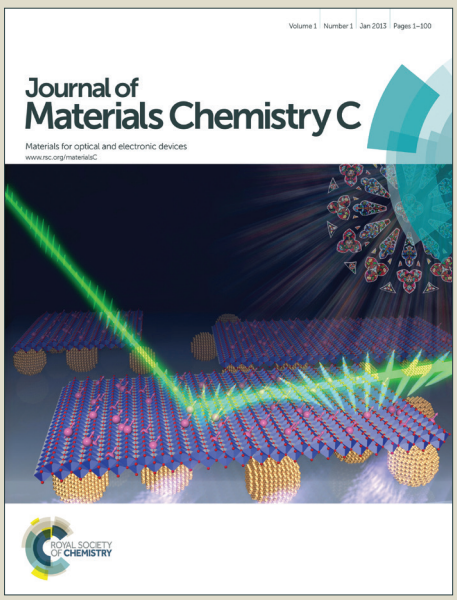

ROYAL SOCIETY OF CHEMISTRY

www.rsc.org/materialsC

White-light-emitting KCl:Eu^{2+}/KCN Crystal for Solid-State lighting devices

Luis Humberto da Cunha Andrade[*a], *Sandro Marcio Lima*[a], *Rogério Ventura da Silva*[a], *Mauro Luciano Baesso*[b], *Yannick Guyot*[c] *and Luiz Antônio de Oliveira Nunes*[d]

[a]Grupo de Espectroscopia Óptica e Fototérmica, Universidade Estadual de Mato Grosso do Sul-UEMS, MS, Dourados, C. P. 351 CEP 79804-970, Brazil.

[b]Departamento de Física, Universidade Estadual de Maringá, Av. Colombo, PR, Maringá, 5790 CEP 87020-900, Brazil.

[c]Laboratoire de Physico–Chimie des Matériaux Luminescents,Université de Lyon,Université Claude Bernard Lyon 1, Villeurbanne, UMR 5620 CNRS 69622, France.

[d]Instituto de Física de São Carlos, Universidade de São Paulo, 400 Av. Trabalhador São-Carlense, 13566-590 São Carlos, SP, Brazil

*E-mail: luishca@me.com

Abstract

The optical and colorimetric properties of a KCl:Eu^{2+}/KCN crystal are analyzed in this paper to verify its potential for the development of white-light-emitting diode (WLED) devices. An unusual broad and intense yellow-green emission band is observed at 530 nm when this crystal is excited with UV radiation. This emission originates from the coupling between the Eu^{2+} ions and multiple the CN^- molecular ions. Luminescence experiments, at middle infrared and visible spectral region, at different temperatures and excitations indicate that both emissions are characteristic of the energy transfer from the Eu^{2+} ions to the CN^- molecular ions. The luminescence quantum efficiency of this material was measured using thermal lens spectroscopy, which provided a high value of ~95%. Based on the experimental results, a model to explain the Eu-CN coupling is proposed. A WLED prototype was constructed using an UV LED to excite the KCl:Eu^{2+}/KCN crystal and using a small amount of Y_2O_3:Eu^{3+} phosphor powder to compensate for the red color. The results showed a correlated color temperature of 3300K; the u', v' color coordinate distance to the Planckian Locus (Du'v') was -0.0008, and the Color Rendering Index (CRI) was approximately 90. These parameters are considered excellent for white light for indoor illumination. Therefore, the results of this work suggest that this crystal is promising for white-light application.

1. Introduction

The new generation of white-lighting-emitting diode (WLED) devices, which are known as light sources constructed from a combination of commercial LEDs with solid state phosphors, has been widely used for indoor and outdoor artificial illumination[1-, 2, 3]. The main challenge of these devices is to replace the traditional fluorescent, incandescent or halogen lamps because

WLEDs are free of mercury in their chemical composition, are highly efficient at converting electrical energy into light and have a long working lifetime (~100,000 hours).[1-4,6]

WLED devices can be fabricated by combining blue or UV LEDs with luminescent materials; this method has low-cost and produces high brightness.[4-6] Many materials have been used to obtain broad emission bands that cover a wide spectral range. However, this type of device often exhibits low Coloring Rendering Index (CRI), and low luminous efficiency mainly because of the difficulties in obtaining red-emission phosphors.[1, 5-8]

A previous study showed intense visible emission as a result of a coupling among the substitutional cyanide (CN^-) radicals, with F color centers.[9,11] Subsequently, similar emission behaviors were observed in the energy transfer mechanisms between metal or rare earth ions and multiples CN^- molecular ions, such as $Yb^{2+}/(CN^-)_n$.[10, 11] Another pair of defects that presented unusual broad and intense visible emission was reported in the $KCl:Eu^{2+}/KCN$ system.[12.] Considering the easy fabrication, high-brightness ability of this material and the great interest in new phosphors for white-lighting application, this work aims to evaluate the broad emission band of this material when it is excited by violet radiation to envision WLED application. A model is presented to explain its broad and intense emission band and its colorimetric properties.

2. Experimental Section

The samples were prepared using the conventional Czochralski method in argon atmosphere. The growth rate was approximately 5 mm/h with a rotation speed of 25 rpm. The double doping was performed with a nominal concentration of 1% $EuCl_3$ and 1% KCN. The obtained crystals were manually cleaved using a still blade along the crystalline plane. Subsequently, the sample

surfaces exhibited good optical quality because there was few crystalline strain caused by plane dislocation or others structural defects that difficult the cleavage of the crystal.

To perform the color compensation in the red region, the Y_2O_3+1 wt% of Eu^{3+} powders were obtained using the spray pyrolysis method. This material was mixed with the powders from the KCl:Eu^{2+}/KCN crystal.

The UV-Vis and IR absorption spectra were obtained using a Perkin Elmer Lambda-900 spectrophotometer, and a Nicolet Magna-850 spectrometer, respectively. Luminescence experiments were performed using a tunable OPO laser or a continuous excitation from a Xe^+ lamp. The emission signal from the sample was collected and focalized in a monochromator Thermo Jarrell-Ash with a diffraction grating of 1800 l/mm and blaze for maximum response at 500 nm. Detection was achieved using a photomultiplier R928. For luminescence experiments at high temperatures, the sample was placed on a copper plate, which was coupled with a 250 W electrical resistance. A chromel-alumel type thermocouple was kept in contact with of the sample surface to monitor temperature (accuracy of 0.5 ˚C). The desired temperature was obtained by controlling the current in the system. The luminescence quantum efficiency was determined using Thermal Lens Spectroscopy (TLS). The details of the experimental setup can be found elsewhere.[13]

After the spectroscopic measurements the KCl:Eu^{2+}/KCN sample were crushed using an agate mortar and pestle to obtain a grain size of approximately 30 μm. A prototype devices of WLEDs were constructed by placing KCl:Eu^{2+}/KCN powder over a commercial violet LED. An optical fiber was used to carry the powder-LED combined emissions to an Ocean Optics HR 4000 spectrometer with a spectral resolution of 1 nm.

3. Results and Discussion

3.1. UV-visible absorption and emission spectra

Figure 1 shows the room-temperature optical absorption (OA) and emission (OE) spectra of the KCl:Eu^{2+}/KCN crystal and emission spectrum of KCl:Eu^{2+} crystal. Two broad absorption bands are observed at 250 and 350 nm from the $4f^7 \rightarrow 4f^6E_g$ and $4f^7 \rightarrow 4f^65T_{2g}$ transitions, respectively[12]. The high absorption coefficient of these bands characterizes the allowed electrical dipole transition.

In KCl the substitutional Eu^{2+} reduces the O_h symmetry to C_{2v} owing the charge compensating cation-vacancy neighboring Eu^{2+} in the <110> direction.[14, 15] Thus, the T_{2g} electronic level should split into three other levels. Because the measurement was performed at room temperature, these OA bands are not well resolved (indicated by arrows). According to the symmetry structure of this crystal, the E_g electronic level of the *d* bands should also be split into two levels. However, because of the strong interaction between the *5d* orbitals and the lattice, particularly in the UV region, these bands cannot be resolved. It is expected that co-doping KCl:Eu^{2+} with KCN, agglomerations of Eu^{2+} with several CN^- molecular ions: Eu^{2+} -$(CN^-)_n$ will be formed, causing a reduction of the C_{2v} symmetry. Thus, the interaction of these molecular ions with Eu^{2+} ions must be considered in this analysis.By comparing the OA spectrum of the KCl that was only doped with Eu^{2+}, which was reported in the literature,[12, 15 -17] it can be noted that the interaction of the $(CN^-)_n$ molecular ion with the Eu^{2+} ions causes a slight effect on the visible OA of this divalent ion, which can be seen as a week shoulder from 450 to 600nm. This behavior was also observed in KCl:Yb^{2+}/KCN^-.[9, 11, 12, 14]

The emission band is broad and covers a wide spectral range from 480 to 620 nm, with a maximum at approximately 530 nm. By changing the excitation spectrum from 320 to 400 nm,

this yellow-green broad emission does not significantly change in terms of position and width. However, under UV excitation, the emission band at 420 nm with a full width at half maximum (FWHM) of 1211 cm^{-1} appears. This emission is attributed to the Eu^{2+} single ions in the crystal and can also be observed in Eu^{2+}-doped KCl samples, as shown in Figure 1. The broad yellow-green emission is attributed to pairs of Eu^{2+} and $(CN^-)_n$ in the crystal, and it is not observed when this sample is only doped with Eu^{2+}.[13, 19] In addition, when the KCl:Eu^{2+}/KCN crystal is submitted to temperature treatment at 830 °C for 30 min and rapidly cooled to room temperature, the centers of the $(CN^-)_n$, $^-$ and Eu^{2+} ions are uncoupled, the yellow-green emission band vanishes, and the only remaining emission band is at 420 nm.[18] Thus, the broad visible emission band observed in Figure 1 originates from the energy transfer from Eu^{2+} to $(CN^-)_n$ The explanation about the observed emission spectrum for KCl:Eu^{2+}/KCl with excitation at 470 nm will be given in following.

3.2. Infrared absorption and emission from CN^- molecular ions

Figure 2 shows the IR absorption (a) and emission (b) spectra of the KCl:Eu^{2+}/KCN^- measured at 300 K. The absorption spectrum exhibits peaks at 2181.8 and 2170.0 cm^{-1}, which are attributed to the symmetric and anti-symmetric stretching modes, respectively, of the OCN^- molecular ions in the crystal.[20] It is important to remember that there are always OCN^- impurities in the crystal that could not be avoided during the sample preparation, however the crystal growth under inert atmosphere prevent avoid formation of OCN^- thus, the concentration of this impurities should be very low compared to CN^- molecular ions. The peaks at 2084 and 2079 cm^{-1} are observed because of the *R* and *P* branches of a free-rotor model, which involves rotational and vibrational modes of the CN^- ions.[9] These peaks overlap with a broad band centered at

2075cm^{-1}, which originated from the coupling between the vibrational modes of CN^- and complex impurities in the host. In addition, by exciting the samples at 355 nm, a broad emission band centered at 2060 cm^{-1} with a full width at half maximum (FWHM) of 76 cm^{-1} can be observed (Figure 2(b)). This excitation energy is not resonant with the CN^- OA but with the Eu^{2+} one. Thus, the observed IR emission spectrum from CN^- molecular ions originates from the energy transfer from Eu^{2+} to $(CN^-)_n$ ions.

Figure 3 shows our proposed scheme for the energy transfer from Eu^{2+} to $(CN^-)_n$ ions. The scheme explains the broad emission bands at 530 nm and in the IR region, both of which are induced by UV, violet or blue excitations. The mechanism predicts that several CN^- ions surrounding the Eu^{2+} ion induce a red shift of its absorption and emission bands. A similar behavior was also observed for KCN:Yb^{2+}/KCN.[14] In this case there are singles Eu^{2+} and clusters of Eu^{2+}-$(CN^-)_n$ in the crystal becoming possible that the excitation at 470nm, which is lower than the energy involving $^8S_{7/2} \rightarrow 4f^6 5T_{2g}$ of alone Eu^{2+} absorption transition, excites these Eu^{2+}-$(CN^-)_n$ clusters. Under this excitation it is observed a yellow–green luminescence centered at 586 nm as observed in Figure 1. The broadening of the emission band is originated from several electronic vibrational (EV) coupling of the Eu^{2+}-$(CN^-)_n$ clusters. In this case the molecule relaxes stepwise down the vibrational ladder; partially radiatively giving rise to vibrational luminescence (VL) in the visible and in the infrared at 2080 cm^{-1}.[11, 14] The CN^- vibrational bands also overlap the excited state band of Eu^{2+} becoming possible that under excitation the lowers states of the vibrational band become populated and thus the transient absorption (TA) promotes again these electros to excited levels. This effect can enhance the optical absorption by a factor more than 20 and these absorption bands should appears at same position of the yellow-green

emission only under excitation.[11] This explains why excitations at lower energy than the $^8S_{7/2} \rightarrow 4f^6 5T_{2g}$ Eu^{2+} transitions, can produce yet the yellow-green emission.

- There are also uncoupled Eu^{2+} ions in the crystal that emits only at 420nm.

3.3. Chromaticity analysis

Figure 1 shows that different excitation wavelengths induce a small displacement in the emission spectra, which indicates that the excitation band responsible for this emission is broad. Furthermore, the optical defect, which is responsible for this broad emission in the visible range, is localized in a specific region in the energy diagram. This characteristic represents an advantage in using this material for a yellow-green-light source under UV-blue LED excitation, where a small change in the excitation wavelength because of a temperature change in the LED junction will not affect the emission spectrum profile. A broad absorption band covering the UV-violet region is interesting for white-light application because excitation sources in this spectral region are easily obtained from commercial GaN-based LEDs.

The observed displacement in the emission can be better visualized in terms of the color coordinates. Figure 4(a) shows the (x, y) coordinates plotted in a CIE 1931 color diagram. When the excitation wavelength is tuned from 360 to 400 nm, the (x, y) coordinates displace towards the border of the color diagram. This displacement under different excitations can be predicted from the emission behavior and the absorption spectra in Figure 1: when the sample is excited in different positions of the absorption band centered at 350 nm, there is a blue emission from the single Eu^{2+} ions that are not paired with CN^- molecular ions. For example, this phenomenon is not observed for excitation at 400 nm. This blue emission contributes to the displacement in the color coordinates towards the central position of the CIE 1931 color diagram and consequently

increases the correlated color temperature (CCT), which is the corresponding black-body color temperature. This behavior is an interesting characteristic of this material because it can avoid high blue or violet color compensation from the LED emission, which must be added to the phosphor yellow-green emission to generate WL. Figure 4(b) shows the CCT values for excitations from 250 to 400 nm. Table 1 shows different colorimetric parameters evaluated for KCl:Eu^{2+}/KCN at different excitations. An important magnitude to evaluate the characteristic of a phosphor for WL application is the distance from the color coordinate position in the CIE 1976 (u', v') color diagram to the nearest position of the Planckian Locus, which is labeled as Du'v'.[21] When the excitation wavelength is changed from UV to violet, the Du'v' value slightly increases. Compared to other studied materials for WL application, such as YAG:Ce^{3+},[22] Sr_3SiO_5:Ce^{3+}, Li^+,[23] LSCAS:Ce/Eu glasses and nitrites,[24, 25] this crystal presents an intermediate Du'v' value that does not significantly change for a large excitation range. However, the CCT values displace more than 1300 K when the excitations vary from 320 to 400 nm, as observed in Figure 4(b).

To evaluate the potential of the KCl:Eu^{2+}/KCN crystal for WLED devices, it is notably important to discuss the temperature dependence of the emission spectra. Figure 5(a) shows the KCl:Eu^{2+}/KCN emission under excitation at 325 nm and different temperatures (from room temperature to ~400 K). At room temperature, the broad emission in the yellow-green region, centered at 550 nm, whose origin was previously discussed in sections 2.1 and 2.2, is more intense than the blue band at 420 nm, which is attributed to the Eu^{2+} ions. By increasing the temperature, the intensities of these two bands invert: the yellow-green band intensity decreases, whereas the blue-band intensity increases. This behavior can be explained by understanding the temperature effect on the pairs of Eu^{2+} and CN^- ions. At relatively low temperatures, the pairs of

Eu^{2+}-$(CN^-)_n$ join together inside the lattice, and the energy transfer from the Eu^{2+} ions occurs as previously discussed and shown in Figure 3. When the sample is heated, the pairs move inside the lattice, and the thermal energy may induce separation of the pairs[26]. In this case, the electronic relaxation of the Eu^{2+} ions occurs without the energy transfer to CN^- ions. Then, the blue emission becomes more intense than the yellow-green emission. Another behavior observed in the luminescence spectra of Figure 5 is that when the temperature increases, the yellow-green emission decreases, and its central position shifts to the blue.

Figure 5(b) shows the thermal dependence of the emission in the visible range. The observed intensity decreases approximately 40% from room temperature to 400 K. This value is an intermediate value compared to the emission of phosphor candidates for WL generation, such as YAG:Ce^{3+},[27] $Ca_2MgSi_2O_7$:Eu^{2+} and (Tb, Gd)AG:Ce^{3+}.[28, 29] This result indicates that the efficiency of the yellow-green emission is inversely proportional to the temperature. Thus, this crystal is not well adapted for high-temperature media. However, for the examined prototypes in section 2.5, the junction temperature from the violet pump LED does not affect the luminescence properties with time. This result indicates that for low-power pump UV or violet LEDs, this temperature dependence is not a drawback for WLEDs.

3.4. Luminescence quantum efficiency of KCl:Eu^{2+}/KCN

The luminescence quantum efficiency (η) of the KCl:Eu^{2+}/KCN crystal was determined using the well-known Thermal Lens (TL) spectroscopy.[16] In this experiment, it is possible to measure the fraction of the absorbed energy by the sample that is converted into heat (φ). Knowing the average emission wavelength ($<\lambda_{em}>$), the technique data can be used to calculate η using the relation $\varphi = 1-\eta(\lambda_{exc}/<\lambda_{em}>)$, where λ_{exc} is the excitation wavelength. In our setup, we used λ_{exc}=

457 nm to excite Eu^{2+}, whose $<\lambda_{em}>$ is ~522 nm. Because φ ~0.17 was measured, η =(95±5)% was determined. In order to check this value we measured a KCl:Eu^{2+} sample and an similar value of $\varphi \sim 0.16$ was measured indicating a high quantum efficiency. This value is similar to the previously measured values for KCl:Eu^{2+} and $SrCl_2$:Eu^{2+}.[30, 31] This high value is expected because the system can be considered a three-level system, so the ground state can be thermally populated at room temperature.[31] Although the low KCN concentration can interfere in the luminescence spectrum the EV energy transfer to the multi CN^- neighbors to Eu^{2+} is efficient. Another evidence that the energy transfer of Eu^{2+}-$(CN^-)_n$ does not decrease the quantum efficiency of KCl:Eu^{2+} can be observed in Figure 5. Increasing the temperature the Eu^{2+}-$(CN^-)_n$ clusters are destroyed remaining the uncoupled Eu^{2+} in the lattice. In this case it can be observed that the increase of the blue emission spectra is proportional to the decease of the green-yellow emission band. This means that the numbers of blue photons converted to yellow ones are proportional.

3.5. Chromaticity analysis for WLED application

Figure 6 shows the scheme of the prototype device that was constructed to observe the colorimetric properties of this crystal when it was excited under UV LED. The spectral resolution was 1 nm. The appropriate Du'v' distances were continuously measured, whereas the crystal phosphor in powder form was added over the LED junction, as represented in Figure 6.

Figure 7(a) shows the obtained spectra for different powder layers (L = 0.2, 0.5, 0.8 and 1.0 mm). The used electrical current was 25 mA. Note that the violet emission spectra from KCl:Eu^{2+}/KCN overlap with the LED excitation. When the layer thicknesses increased, the transmission intensity of the violet and LED emissions became less intense because of the down

conversion to the yellow-green-color effect. The color appearance is represented in terms of the (x, y) position on the CIE 1931 color diagram, as illustrated in Figure 7(b).

A color displacement can be noted when the phosphor layer thickness increased, which increased the Du'v' values and consequently lowered the CCT numbers, as shown in Table 2. The observed Du'v' values are higher than 0.006, which is the maximum value accepted by the American National Standards Institute (ANSI C-78.377). However, the LED prepared with a phosphor layer of 0.2 mm provided a CCT of 5950 K and a Du'v' of 0.019, which are acceptable values by other standards, such as the Japanese Standard Association (JIS C-8152-2), which defines the limit of |Du'v'| to be <0.02.

The WLED constructed as described in Figure 6 presents a parallel increase of the transmission intensity of the 405 nm band from the excitation LED, as shown in Figure 8. This result indicates that for this current range, the mentioned parameters, such as Du'v', CCT and the colorimetric coordinates, remain constant for different LED intensities. Despite these attractive characteristics for LED application, the results indicate that this phosphor lacks red emission, which results in a high CCT value for the smallest target Du'v'. Figure 7(b) shows that if the red colors of the emission spectra were increased, the CCT and the Du'v' values would decrease, and the CRI values would increase. An alternative method to achieve this is to add an efficient red-emission phosphor, such as the $Y_2O_3:Eu^{3+}$ crystal, which is an interesting phosphor material that has been extensively used for this purpose in several devices, such as displays and fluorescent lamps.[31] $Y_2O_3:Eu^{3+}$ presents a strong red luminescence with high quantum efficiency.[32]

Figure 9(a) shows the emission spectra of the $KCl:Eu^{2+}/KCN$ crystal with the appropriate amount of $Y_2O_3:Eu^{3+}$ pounders, which were obtained for the 405 nm violet LED excitation. The

$Y_2O_3:Eu^{3+}$ pounder presents several narrow emission lines from 580 to 711 nm, with the strongest one at 611 nm. The emission color coordinates that correspond to the Planckian Locus are shown in the CIE 1976 u'v' color diagram in Figure 9(b). It can be observed that when both phosphors are mixed, it is possible to obtain an optimum displacement to the Planckian Locus, as shown in the color diagram. All color coordinates generated from the spectra, as shown in Figure 9(a), are less than 0.004 from the Planckian Locus. The CCT values can change depending on the thickness of the phosphor layer, the amount of $Y_2O_3:Eu^{3+}$ mixed with $KCl:Eu^{2+}$/KCN crystals, as shown in Table 3, jointly with the nearest standard illuminate source and the CRI values. In general, the ANSI considers a source to be acceptable for indoor illumination if the CRI is ~70, whereas values close to 80 are considered good, and 90 is excellent. The present case illustrates that an appropriate CRI for indoor illumination can be obtained by mixing $KCl:Eu^{2+}$/KCN crystals with $Y_2O_3:Eu^{3+}$. These values are similar to those of some efficient fluorescent lamps and WL obtained using three or even four color LED devices.[33, 34, 35]

4. Conclusion

The broad yellow-green emission band observed in the $KCl:Eu^{2+}$/KCN samples originates from the energy transfer from Eu^{2+} ions to CN^- molecular ions. This effect was confirmed by observing the infrared emission under UV or violet excitation. The energy transfer from Eu^{2+} to CN^- depends on the excitation wavelength and induces an effect of color temperature tuning, which is interesting for WL application. This crystal presents many interesting advantages for phosphor devices, such as cheap and easy fabrication, high luminescence quantum efficiency and high appropriate color temperature. High values of CRI (close to 90) were obtained by mixing the powders of $KCl:Eu^{2+}$/KCN and $Y_2O_3:Eu^{3+}$ and combining the mixture with violet LED

emission. Beyond the WL application shown in this manuscript, the intense and efficient yellow-green emission under UV or violet excitation can be applied for UV-Vis down-conversion systems, which can be used to increase the optical response of visible-light detectors.

Prototype devices of WLEDs were constructed by placing KCl:Eu^{2+}/KCN powder over a commercial violet LED. An optical fiber was used to carry the powder-LED combined emissions to an Ocean Optics HR 4000 spectrometer with a spectral resolution of 1 nm.

4 Acknowledgments

The authors thank the CAPES/COFECUB Brazil/France cooperation Grant No. 565/07, FundaçãoAraucária, CNPq, FINEP and CNRS-UCB Lyon 1 for their financial support.

5. References

1 E. F. Schubert and J. K. Kim, *Science,* 2005, **308**, 1274.

2 A. Bierman, *Lighting Research & Technology*, 2012, **44**, 449.

3 M. C. Wei and K. W. Houser, *Leukos*, 2012, **8**, 237.

4 Z. Lei, G. Xia, L. Ting, G. Xiaoling, L. Qiao Ming and S. Guangdi, *J. Microelectr.,* 2007, **38**, 1.

5 J. Hou, W. Jiang, Y. Fang and F. Huang J., *Mater. Chem.* C, 2013, **1**, 5892.

6 X. Zhang, Z. Zhao, X. Zhang, A. Marathe, D. B. Cordes, B. Weeks and J. Chaudhuri, J. Mater. Chem. C, 2013, **1**, 7202.

7 C. Feldmann, T. Jüstel, C. R. Ronda and P. J. Schmidt, *Adv. Funct. Mater*., 2003, **13**, 511.

8 H. S. Jang, W. B. Im, D. C. Lee, D. Y. Jeon and S. S. Kim, *J. Lumin.,* 2007, **126**, 371.

9 W. Gellermann, Y. Yang and F. Luty, *SPIE,* 1986, **622**, 151.

10 M. Muller, J. L. Fabris, A. C. Hernandes and M. Siu Li, *J. Lumin.,* 1994, **59**, 289.

11 V. Dierolf, J. Hoidis, D. Samiec and W. von der Ostern, *J. Lumin.,* 1998, **76&77**, 581.

12 F. M. M. Yasuoka, J. C. Castro and L. A. O. Nunes, *Phys. Rev. B,* 1991, **43**, 9295.

13 G. H. Muñoz, L. C de la Cruz, F. A. Muñoz, O. J. Rubio, *J. Mater. Sci. Lett.,* 1998, **7**, 1310.

14 C. P. An, V. Dierolf, and F. Luty, *Phys. Rev. B,* 2000, **61**, 6565.

15 W. E. Bron and W. R. Heller *Phys. Rev.,* 1964, **136**, A1433.

16 S. M. Lima, J. A. Sampaio, T. Catunda, A.C. Bento L. C. M. Miranda and M. L. Baesso, *J. Non-Cryst. Solids,* 2000, **273**, 215.

17 I. A. Carcer, F. Cusso and F. Jaque, *Phys. Rev. B,* 1988, **38**, 10812.

18 J. A. Hernandez, W. K. Cory and J.O.Rubio, *J. Chem. Phys*., 1980, **72**, 198.

19 J. P. Driewer, H. Chen, A. Osvet, D. A. Low, H. H. Li, *Med Phys*., 2011, **38**, 4681.

20 H. Huang, K. Alvarez, Q. Lui, T. M. Barnhart, J. P. Snyder and J. E. Penner-Hahn, *J. Am. Chem. Soc.,* 1996, **118**, 8808.

21 L. H. C. Andrade, S. M. Lima, M. L. Baesso, A. Novatski, J. H. Rohling, Y. Guyot, and G. Boulon, *J. Alloys Compd.,* 2012, **510**, 54.

22 Y. Pan, M. Wu, and Q. Su, *J. Phys. Chem. Solids,* 2004, **65**, 845.

23 H. S. Jang and D. Y. Jeon, *Appl. Phys. Lett.,* 2007, **90**, 041906.

24 A. C. P. Rocha, L. H. C. Andrade, S. M. Lima, A. M. Farias, A. C. Bento, M. L. Baesso, Y. Guyot and G. Boulon, *Opt. Express,* 2012, **20**, 10034.

25 R. J. Xie, N. Hirosaki, Y. Li and T. Taked, *Mater.*, 2010, **3**, 3777.

26 F. M. Matinaga, L. A. Nunes, A. C. Zilio and J. C. Castro, *Phys. Rev. B.* 1988, **37**, 993.

27 V. Bachmann, C. Ronda and A. Meijerink, *Chem. Mater*., 2009, **21**, 2077.

28 M. Zhang, J. Wang, W. Ding, Q. Zhang and Q. Su, *Opt. Mater.,* 2007, **30**, 571.

29 A. A. Setlur, W. J. Heward, Y. Gao, A. M. Srivastava, R. G. Chandran and M. V. Shankar, *Chem. Mater*., 2006, **18**, 3314.

30 E. Rodriguez, L. Núñez, J. O. Tocho and F. Cussó, *J. Lumin.,* 1994, **58**, 353.

31 T. Kobayasi, S. Mroczkowski and J. F. Owen, *J. Lumin.,* 1980, **21**, 247.

32 C. Hee Lee, K. Y. Jung, J. G. Choi and Y. C. Kang, *Mater. Sci. Eng. B*, 2005, **116**, 59.

33 G. Blasse and B. C. Grabmaier, Luminescent Materials, Springer-Verlag: New York, **1994**.

34 M. M. Aman, G. B. Jasmon, H. Mokhlis and A. H. A. Bakar, *Energy Policy*, 2013, **52**, 482.

35 S. Muthu, F. J. P. Schuurmans, and M. D. Pashley, *IEEE J SEL TOP QUANT*, 2002, **8**, 333.

Table 1. Colorimetric parameter data for KCl:Eu^{2+}/KCN at different excitation levels.

λ_{exc}(nm)	x	y	u'	v'	Du'v'	CCT
250	0.30	0.43	0.16	0.51	0.061	6200
280	0.32	0.44	0.17	0.52	0.056	5650
300	0.33	0.46	0.17	0.53	0.061	5450
320	0.30	0.43	0.16	0.51	0.060	6350
350	0.31	0.46	0.16	0.52	0.066	5750
370	0.32	0.47	0.16	0.53	0.067	5550
390	0.34	0.48	0.17	0.53	0.068	5200
395	0.34	0.49	0.17	0.54	0.069	5100
400	0.34	0.50	0.17	0.54	0.070	5050

Table 2. Colorimetric parameter data for the KCl:Eu^{2+}/KCN crystal for different layers and an electrical current of 25 mA.

L(mm)	x	y	u’	v’	Du’v’	CCT (K)
0.2	0.33	0.37	0.20	0.49	0.019	5950
0.5	0.35	0.44	0.19	0.52	0.044	5000
0.8	0.36	0.47	0.18	0.53	0.054	4750
1.0	0.38	0.50	0.18	0.55	0.063	4400

Table 3. Color diagram data for the KCl:Eu^{2+}/KCN crystal with the Y_2O_3:Eu^{3+} phosphor.

L (mm)	$xY_2O_3:Eu^{3+} + (1-x)KCl:Eu^{2+}/KCN$ x % =	Du'v'	CRI (Ra)	CCT (K)
0.2	5	-0.0030	88	3770
0.5	10	-0.0008	88	3312
0.8	20	-0.0012	84	2711

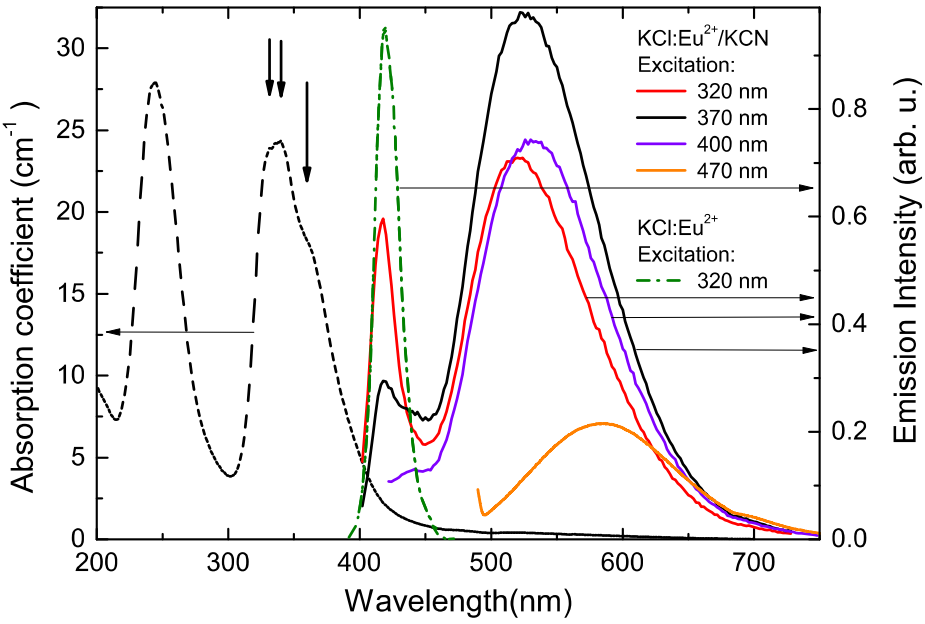

Figure 1. Optical absorption of KCl:Eu^{2+}/KCN and emission spectra of KCl:Eu^{2+}/KCN and KCl:Eu^{2+} measured at room temperature.

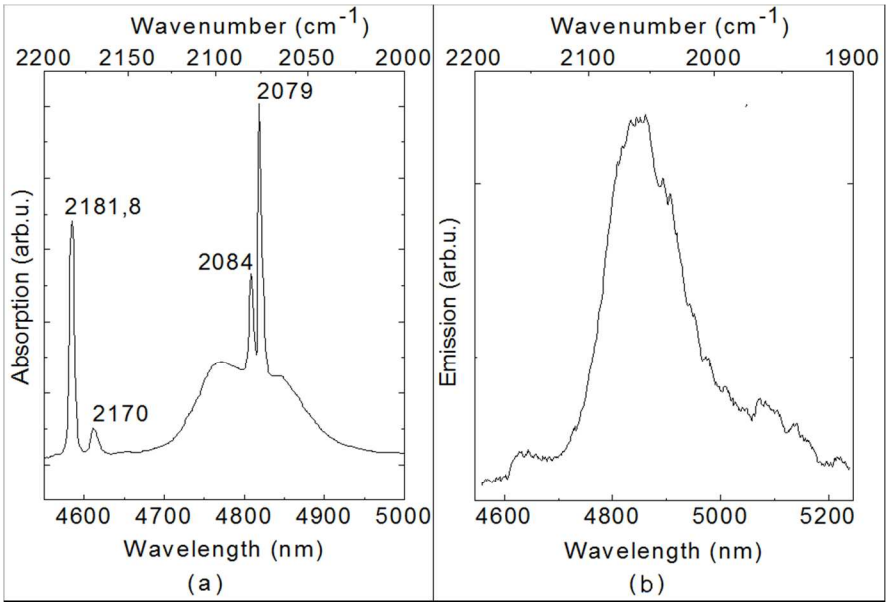

Figure 2. Infrared absorption (a) and emission (b) spectra of KCl:Eu^{2+}/KCN^{-} measured at 300 K. The emission was induced by exciting the crystal at 355 nm.

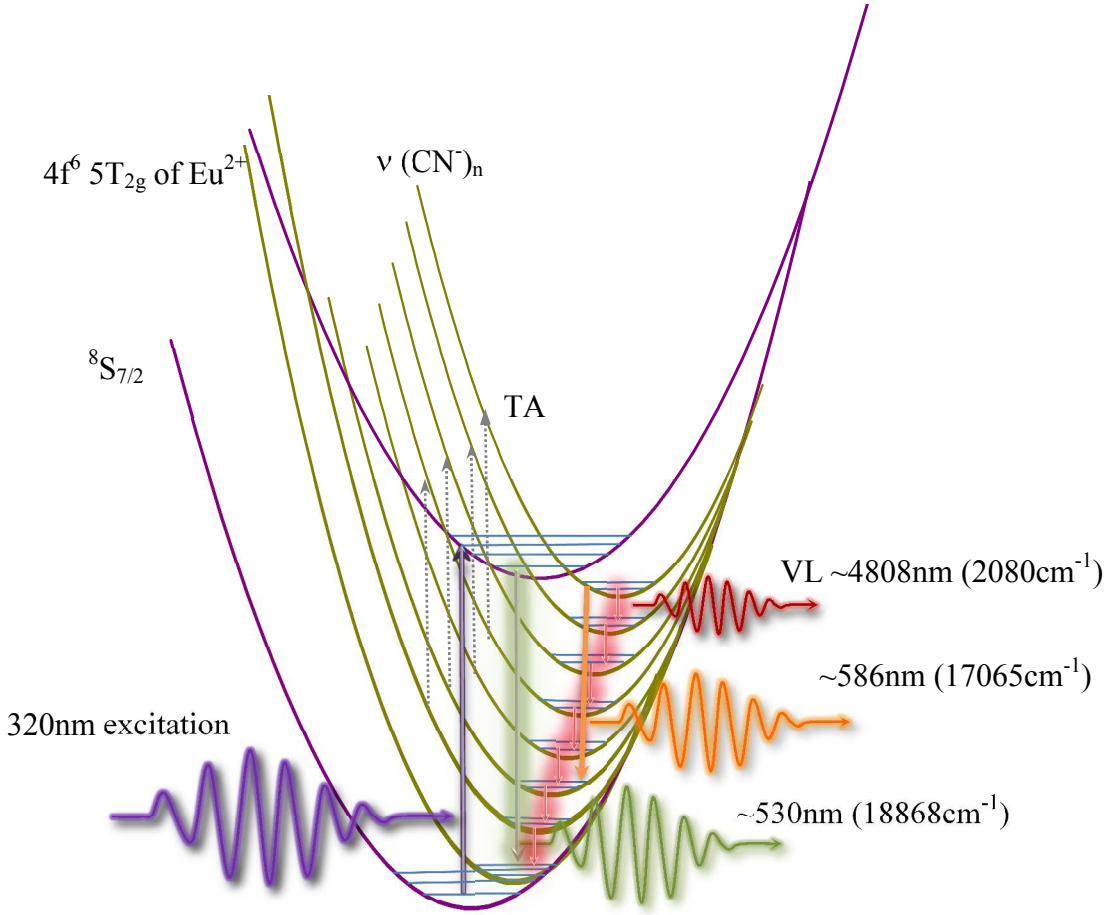

Figure 3. Scheme of the energy transfer from Eu^{2+} to $(CN^-)_n$ ions.

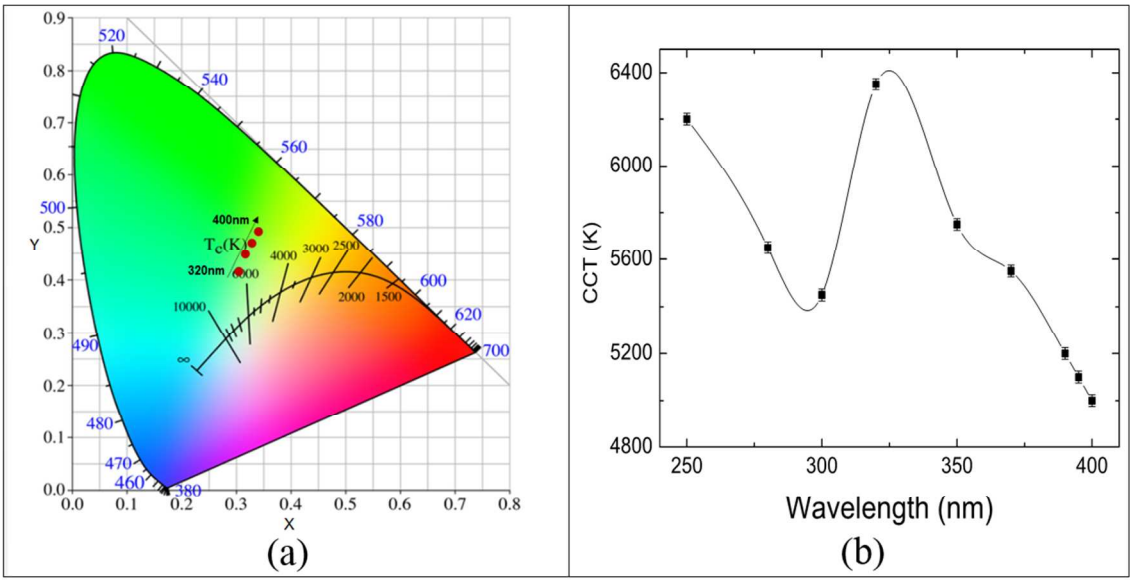

Figure 4. CIE 1931 color diagram (a) and the wavelength dependence of the correlated color temperature (CCT), which corresponds to the black-body color temperature (b).

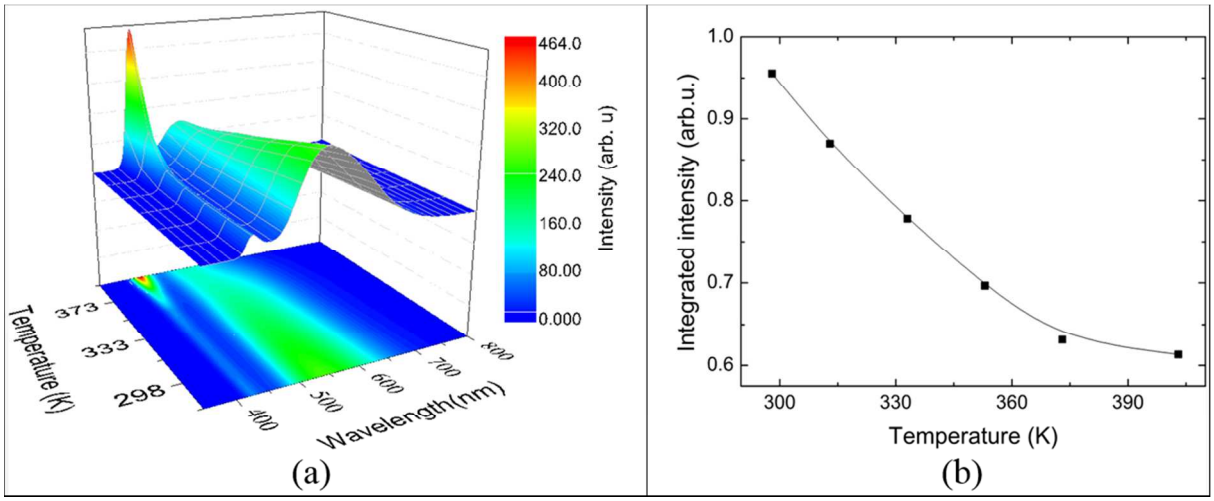

Figure 5. (a) Emission plot for the KCl:Eu^{2+}/KCN crystal as a function of temperature for excitation at 325 nm. (b) Integrated intensity of the yellow emission as a function of temperature.

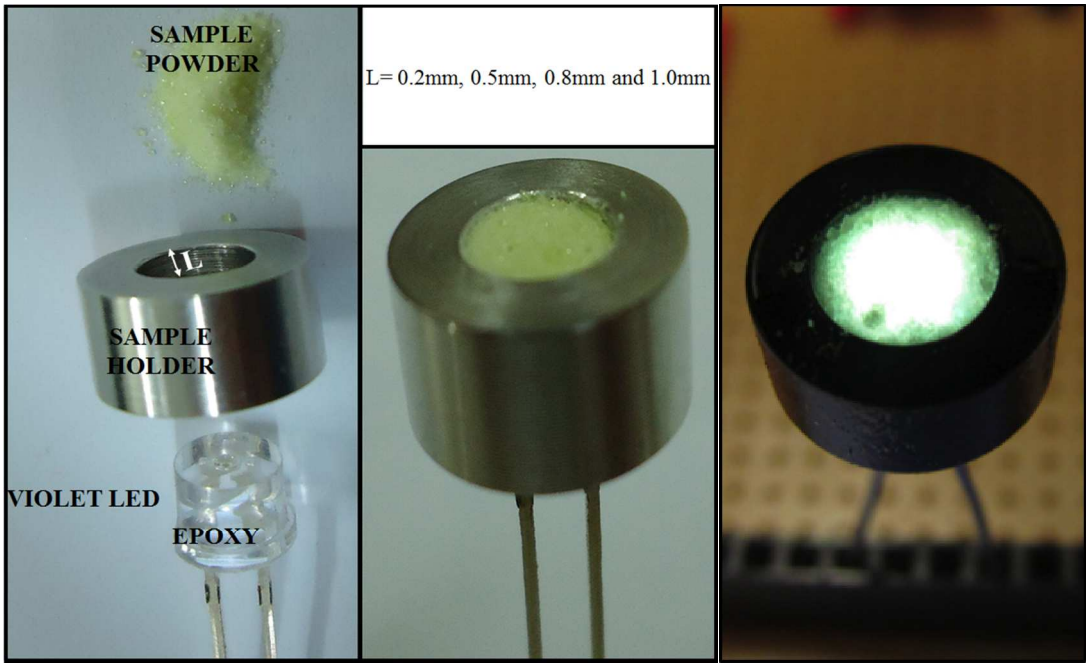

Figure 6. Experimental arrangement to generate WL using LEDs.

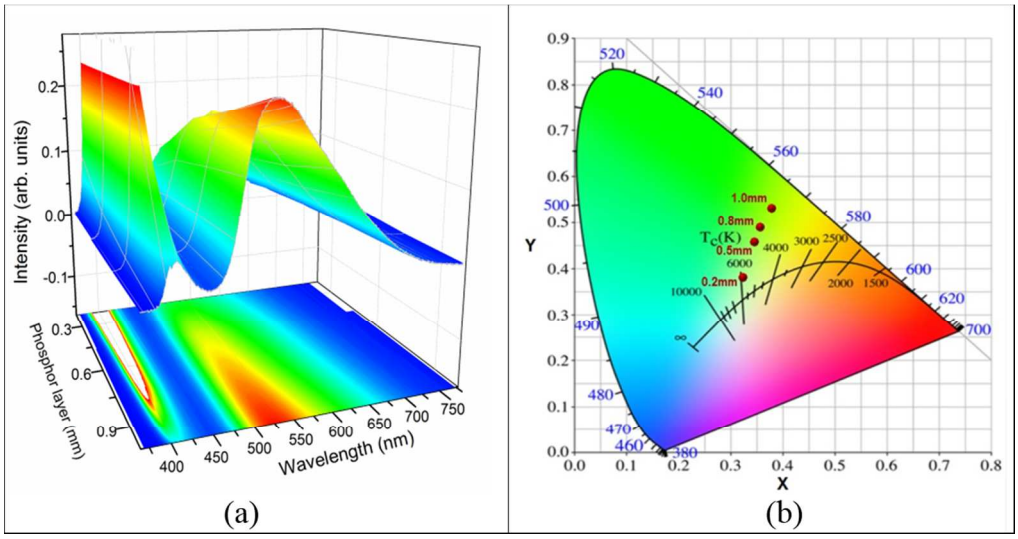

Figure 7. (a) Emission plot for the KCl:Eu^{2+}/KCN crystal as a function of the phosphor layer thickness (0.2, 0.5, 0.8 and 1.0 mm) with excitation at 405 nm. (b) CIE 1931 color diagram for different phosphor layers.

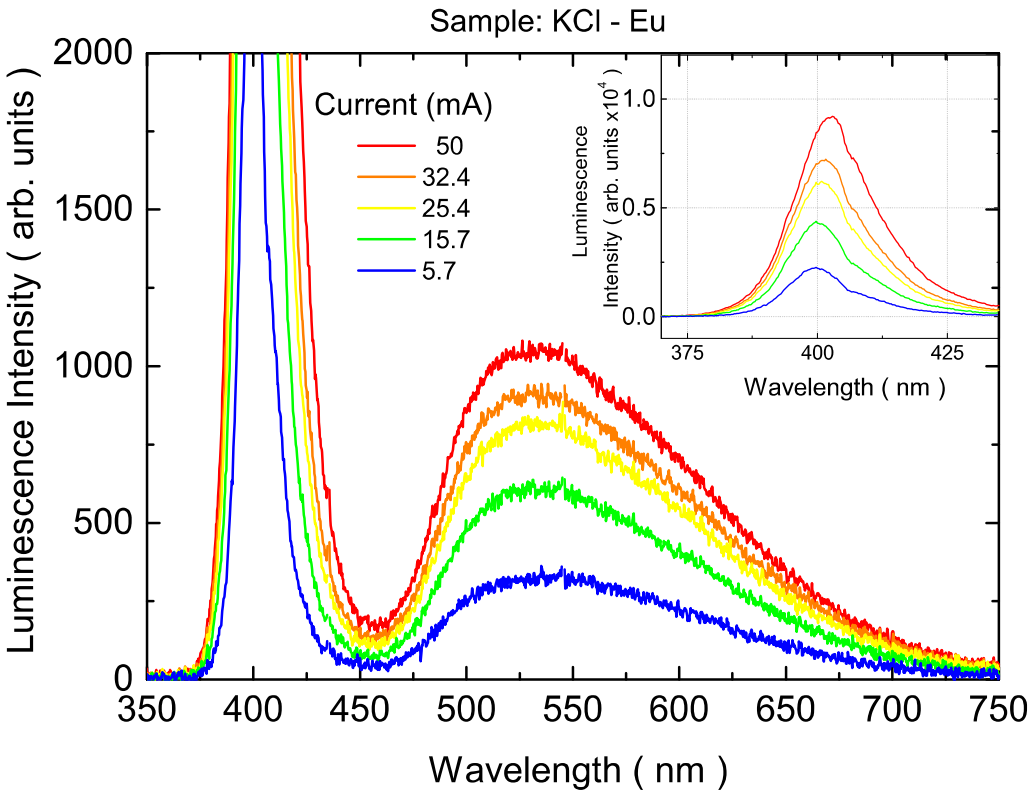

Figure 8. KCl:Eu^{2+}/KCN crystal emission spectra measured for different electrical currents of the LED and with a phosphor layer of 0.2 mm.

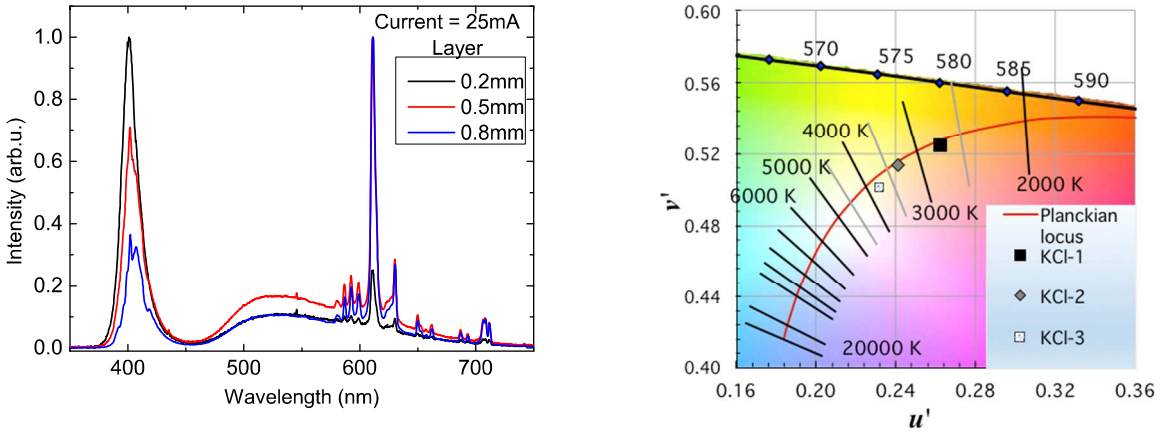

(a) (b)

Figure 9. Emission spectra of KCl:Eu^{2+}/KCN crystals with Y_2O_3:Eu^{3+} under 405 nm violet LED excitation (a) and the CIE 1976 u'v' color diagram (b).

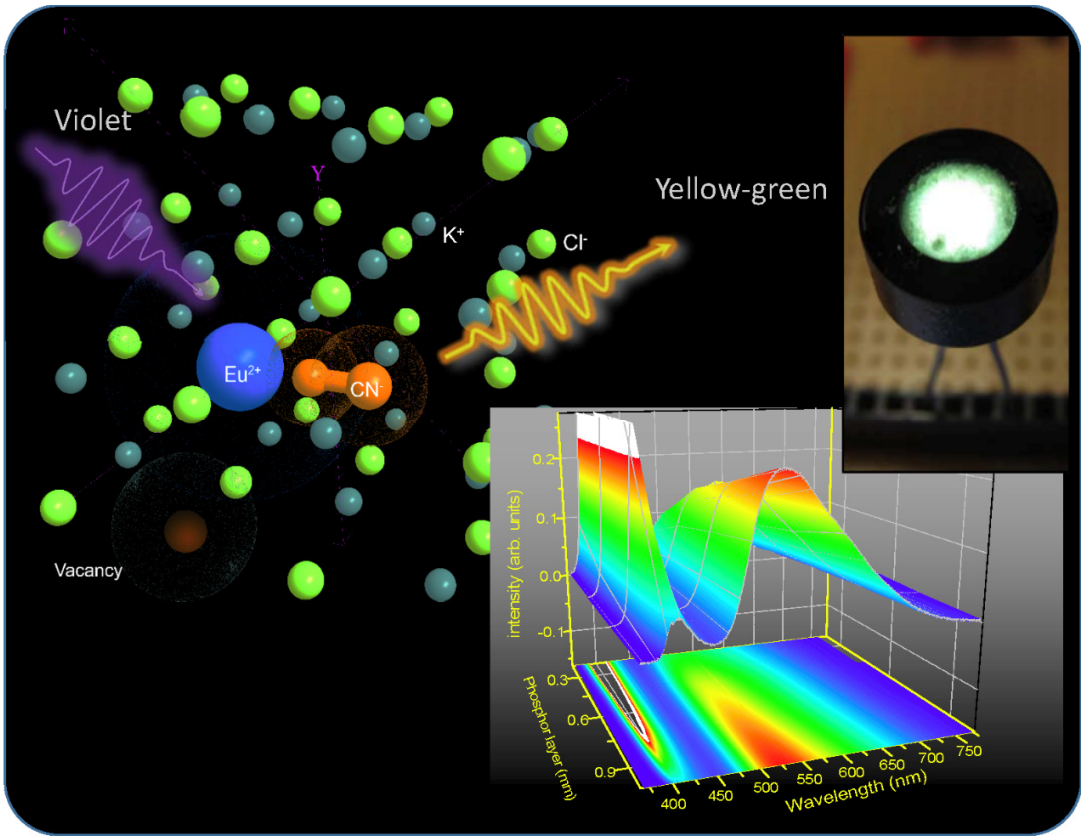

Abstract figure